Article

Hydration Contributions to Association in Polyelectrolyte Multilayers and Complexes: Visualizing Hydrophobicity

Joseph B. Schlenoff, Amir H. Rmaile, and Claudiu B. Bucur

J. Am. Chem. Soc., **2008**, 130 (41), 13589-13597 • DOI: 10.1021/ja802054k • Publication Date (Web): 18 September 2008

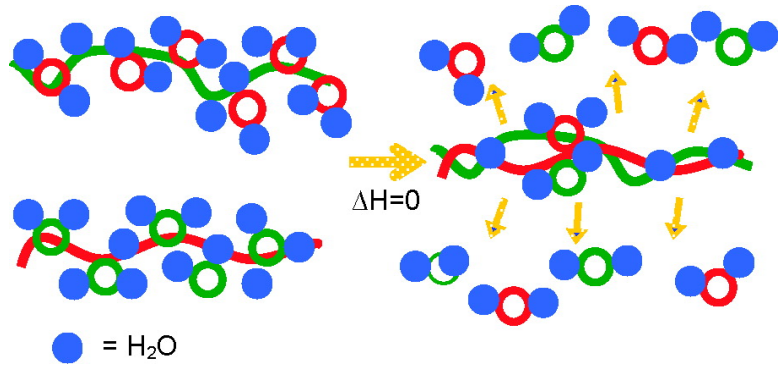

J|A|C|S
ARTICLES

Published on Web 09/18/2008

Hydration Contributions to Association in Polyelectrolyte Multilayers and Complexes: Visualizing Hydrophobicity

Joseph B. Schlenoff,* Amir H. Rmaile, and Claudiu B. Bucur

Department of Chemistry and Biochemistry, The Florida State University, Tallahassee, Florida 32306

Received March 19, 2008; E-mail: schlen@chem.fsu.edu

Abstract: Thin films of polyelectrolyte complex were assembled using the multilayering method with direct, *in situ* observation of all multilayer components using attenuated total internal reflectance FTIR (ATR-FTIR). Buildup and ion doping of two representative combinations of positive and negative polyelectrolytes are controlled by salt type. The internal hydration of multilayers, measured precisely by ATR-FTIR, depends on the chemical identities of the polymers and the salt ions. The efficiency of doping inversely tracks the degree of hydration: less hydrated ("hydrophobic") ions are more efficient dopants, and less hydrated polyelectrolye complexes are harder to dope. Given that polyelectrolyte complexation is essentially entropy-driven, driving forces for doping, or association (the inverse of doping), are rationalized by counting all species in the condensed polyelectrolyte phase, including water molecules. For any combination of uni-univalent salt ions and polyelectrolyte, the strength of polyelectrolyte association is described by a single universal parameter. The magnitudes of the interactions per repeat unit are not high—a few *kT*—and are proportional to the number of water molecules released from the polymers when they form ion pairs. Hydration within multilayers due to residual salt is extensive but may be removed by an external osmotic stressing agent.

Introduction

Although it was expected that molecules of low polarity should experience a free energy penalty on dissolution in water, the finding that their entropic component of hydration often far outweighs the enthalpic one stimulated much interest in the special properties of water.[1−4] The generally accepted model of hydrophobic hydration invokes a cage of water molecules around the nonpolar solute molecule. Hydrogen bonds are preserved by partial ordering of water (a decrease in entropy), and contact with the solute can generate favorable, though small, enthalpies of dissolution. Hydrophobic interactions (also termed "bonding") are generated when multiple nonpolar solutes, or fragments of molecules, associate to maximize contact of water with water, maintaining structure and hydrogen bonds. Multiple, relatively weak, hydrophobic interactions are crucial to protein folding.[5,6]

In a related phenomenon, it has been recognized that desolvation of interacting sites between molecules enhances their binding due to the concomitant increased entropy.[7,8] This entropically driven enhancement of association is, of course, especially significant when the enthalpic contribution is small.[3,8,9] Since water is concentrated around ionic functionality, ion pairing may be highly programmed by chemical design: the more water released, the stronger the pairing. In contrast to classic hydrophobic interactions, the desolvation mechanism relies only on increased entropy by release of water, without reference to additional structuring. Because proteins are charged, and because they exhibit much intra- and extra-molecular ion pairing, it is reasonable to suggest that ion pairing and hydrophobic interactions work cooperatively. That is, when ion pairing is the site of interaction, the "hydrophobicity" of the immediate molecular environment controls the amount of water loss and (re)structuring.

We have recently shown, quantitatively, that ion pairing interactions between synthetic polyelectrolytes of opposite charge, yielding polyelectrolyte complexes (PECs), are essentially driven by entropy.[10] Formation of complex, Pol^+Pol^-, is represented by eq 1,

$$Pol^+A^- + Pol^-M^+ \rightleftharpoons Pol^+Pol^- + A^- + M^+ \qquad (1)$$

where Pol^+A^- and Pol^-M^+ are polycation and polyanion repeat units compensated respectively by negative and positive coun-

(1) Finney, J. *NATO Sci. Ser. Ser. A. Life Sci.* **1999**, *305*, 115–124.
(2) (a) Nemethy, G. *Angew. Chem., Int. Ed. Engl.* **1967**, *6*, 195–206. (b) van Oss, C. J. *J. Mol* **2003**, *16*, 177–190. (c) Akiyoshi, K. *Supramol. Des. Biol. Appl.* **2002**, 13–24.
(3) Paulaitis, M. E.; Garde, S.; Ashbaugh, H. S. *Curr. Opin. Colloid Interface Sci.* **1996**, *1*, 376–383.
(4) (a) Scheraga, H. A. *Biomol. Struct. Dyn.* **1998**, *16*, 447–460. (b) Southall, N. T.; Dill, K. A.; Haymet, A. D. J. *J. Phys. Chem. B* **2002**, *106*, 521–533. (c) ten Wolde, P. R. *J. Phys.: Condens. Matter* **2002**, *14*, 9445–9460.
(5) (a) Stites, W. E. *Chem. Rev.* **1997**, *97*, 1233–1250. (b) Attard, P. *J. Phys. Chem.* **1989**, *93*, 6441–6444.
(6) Hartman, K. A., Jr. *J. Phys. Chem.* **1966**, *70*, 270–276.
(7) (a) Rekharsky, M.; Inoue, Y.; Tobey, S.; Metzger, A.; Anslyn, E. *J. Am. Chem. Soc.* **2002**, *124*, 14959–14967. (b) Mahtab, R.; Harden, H. H.; Murphy, C. J. *J. Am. Chem. Soc.* **2000**, *122*, 14–17.
(8) Rekharsky, M.; Inoue, Y. *J. Am. Chem. Soc.* **2000**, *122*, 10949–10955.
(9) Berger, M.; Schmidtchen, F. P. *J. Am. Chem. Soc.* **1999**, *121*, 9986–9993.
(10) Bucur, C. B.; Sui, Z.; Schlenoff, J. B. *J. Am. Chem. Soc.* **2006**, *128*, 13690–13691.

terions. PECs have been known for many decades, and it was recognized early that their formation is driven by the release of counterions on polymer chains.[11,12] It was also known that complexes exhibit a variety of properties depending on their composition, and that swelling, or "doping", of complexes by addition of salt (the reverse of eq 1) depends on the salt type.[13] We accounted for these differences in terms of the hydrophobicities of the polyelectrolytes or the salt ions employed.[14−17] The spectrum of swelling responses in various salts was recently rationalized[18] using the Hofmeister series.[19,20]

When PECs are formed layer by layer, yielding ultrathin polyelectrolyte "multilayers" (PEMUs),[12,21] both the buildup and the properties of the PEMU depend on counterions.[14,22] The addition of salt to solutions of polyelectrolytes causes them to interact more weakly during buildup,[15] resulting in thicker films.[23] Doping of PEMUs causes a significant and reversible decrease in their elastic modulus, as ion pair cross-links are broken,[22] with differences in modulus noted for different ions.[24]

In this work, we focus on the definition of hydrophobicity[4] and how a quantitative measure of this parameter may be established. Our definition relies on observing the number of water molecules within the condensed PEC phase, which is formed by the multilayering method. The use of attenuated total internal reflectance FTIR (ATR-FTIR)[25] spectroscopy permits unequivocal and accurate counting of water molecules in the complex[26] (which is not possible for bulk solution).

The use of synthetic polyelectrolytes, as opposed to biological ones such as proteins, simplifies the system considerably. First, the former are much less heterogeneous, chemically and structurally, than the latter. Complexes of polyelectrolytes, including those in the PEMU morphology, are widely known to be amorphous,[11a,21] justifying mean-field descriptions of them. Second, the unfolding of a protein is accompanied by a significant increase in configurational entropy, whereas most synthetic polyelectrolytes are not highly structured. In fact, we have demonstrated that enthalpy of mixing (association) of polyelectrolyte complexes decreases as the solutions approach their θ condition (i.e., high salt concentration).[10,26] In our interpretation ideal random coils of unperturbed dimension in solution become incorporated into complexes as random coils of unperturbed dimension. Only a very small loss in translational entropy occurs. Variables include the chemical composition of the PEC and the salt ions, with a broad selection of the latter easily available.

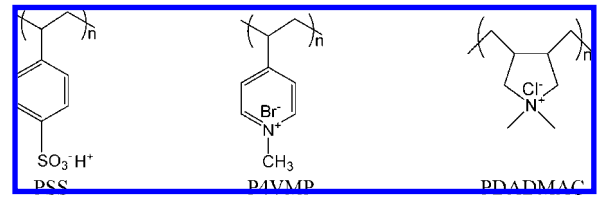

Figure 1. Polyelectrolytes used in the layer-by-layer deposition sequences. From left to right, poly(styrene sulfonic acid), poly(4-vinylmethylpyridinium bromide), and poly(diallyldimethylammonium chloride).

Experimental Section

Materials. All chemicals were used as received unless otherwise specified. The following polymers were used: poly(diallyldimethylammonium chloride) (PDADMAC, Aldrich, M_w=3.69 × 10^5, M_w/M_n= 2.09); poly(styrene sulfonate) (PSS, Aldrich, M_w = 5.75 × 10^4, M_w/M_n= 1.4); poly(ethylene glycol) (PEG, Sigma, M_n = 8000); and poly(4-vinylmethylpyridinium bromide) (P4VMP, Polysciences, M_w = 65 500). Salts were obtained from Fisher Scientific: sodium chloride (NaCl), sodium fluoride (NaF), sodium iodide (NaI), sodium bromide (NaBr), sodium azide (NaN_3), sodium thiocyanide (NaSCN), sodium nitrate ($NaNO_3$), sodium perchlorate ($NaClO_4$), lithium chloride (LiCl), potassium chloride (KCl), cesium chloride (CsCl), calcium chloride ($CaCl_2$), magnesium chloride ($MgCl_2$), and yttrium chloride (YCl_3). Solutions were prepared with 18 MΩ deionized water. Accurate concentrations of salt solutions were determined using conductivity measurements and comparing to tabulated conductivity values.[27] Structures of polyelectrolytes used are shown in Figure 1.

Instrumentation. ATR measurements were performed with a Nicolet Nexus 470 FTIR fitted with a 0.5 mL flow-through ATR assembly housing a 70 × 10 × 6 mm, 45° germanium crystal (Specac Benchmark). The crystal was cleaned using 50:50 v/v ethanol/H_2O in saturated NaCl solution with sonication for 20 min. The crystal was then washed with 18 MΩ deionized water and dried with a stream of nitrogen. PEMU deposition on the Ge crystal was carried out by flowing polyelectrolyte solutions (10 mM polymer concentration based on the repeat unit) in 1.0 M NaCl in an alternating manner through the ATR housing assembly with 1.0 M NaCl rinse solution in between. Films were then annealed with 1.0 M NaCl for 1 week.[28,29] The deposition time for each layer was 5 min. The rinse time was 1 min.

Fourteen different salts were employed to prepare solutions of varying concentration, to which multilayers were exposed. The flow-through cell was typically rinsed with several cell volumes of salt solution, and FTIR spectra were monitored until the system had equilibrated. An equilibration period of 30 min was usually sufficient. An "osmotic stress" [30] experiment exposed PEMU thin films to aqueous PEG solutions ranging in concentration from 0 to 30% by weight. PEG solutions also contained either 10 mM (i.e., a minimal, yet defined, concentration) or 0.5 M NaCl.

(11) (a) Bixler, H. J.; Michaels, A. S. *Encycl. Polym. Sci. Technol.* **1969**, *10*, 765–780. (b) Michaels, A. S.; Mir, L.; Schneider, N. S. *J. Phys. Chem.* **1965**, *69*, 1447–1455.
(12) Decher, G.; Schlenoff, J. B. *Multilayer thin films: sequential assembly of nanocomposite materials*; Wiley-VCH: Weinheim, Germany, 2003.
(13) (a) Michaels, A. S.; Miekka, R. G. *J. Phys. Chem.* **1961**, *65*, 1765–1773. (b) Michaels, A. S. *J. Ind. Eng. Chem.* **1965**, *57*, 32–40. (c) Hatch, M. J.; Dillon, J. A.; Smith, H. B. *Ind. Eng* **1957**, *49*, 1812–1819. (d) Yano, O.; Wada, Y. *J. Appl. Polym. Sci.* **1980**, 1723–1735.
(14) Dubas, S. T.; Schlenoff, J. B. *Macromolecules* **1999**, *32*, 8153–8160.
(15) Farhat, T. R.; Schlenoff, J. B. *Langmuir* **2001**, *17*, 1184–1192.
(16) Farhat, T. R.; Schlenoff, J. B. *J. Am. Chem. Soc.* **2003**, *125*, 4627–4636.
(17) Schlenoff, J. B., Chapter 4 in ref 12.
(18) Salomäki, M.; Tervasmäki, P.; Areva, S.; Kankare, J. *Langmuir* **2004**, *20*, 3679–3683.
(19) Hofmeister, F. *Arch. Exp. Pathol. Pharmakol.* **1888**, *24*, 247–260.
(20) Cacacem, M. G.; Landau, E. M.; Ramsden, J. J. *Q. Rev. Biophys.* **1997**, *30*, 241–277.
(21) (a) Decher, G. *Science* **1997**, *277*, 1232–1237. (b) Lösche, M.; Schmitt, J.; Decher, G.; Bouwmann, W. G.; Kjaer, K. *Macromolecules* **1998**, *31*, 8893–8906.
(22) Jaber, J. A.; Schlenoff, J. B. *J. Am. Chem. Soc.* **2006**, *128*, 2940–2947.
(23) Schlenoff, J. B.; Dubas, S. T. *Macromolecules* **2001**, *34*, 592–598.
(24) Salomäki, M.; Laiho, T.; Kankare, J. *Macromolecules* **2004**, *37*, 9585–9590.
(25) (a) Sukhishvili, S. A.; Granick, S. *Macromolecules* **2002**, *35*, 301–310. (b) Harrick, N. J. *Internal reflection spectroscopy*; Interscience: New York, 1967. (c) Urban, M. W. *Attenuated internal reflectance spectroscopy of polymers*; American Chemical Society: Washington, DC, 1996.
(26) Jaber, J. A.; Schlenoff, J. B. *Macromolecules* **2005**, *38*, 1300–1306.
(27) Dobos, D. *Electrochemical data; a handbook for electrochemists in industry and universities*; Elsevier SPC: New York, 1975.
(28) Dubas, S. T.; Schlenoff, J. B. *Langmuir* **2001**, *17*, 7725–7727.
(29) Jomaa, H. W.; Schlenoff, J. B. *Macromolecules* **2005**, *38*, 8473–8480.
(30) Leonard, M.; Hong, H.; Easwar, N.; Strey, H. H. *Polymer* **2001**, *42*, 5823–5827.

Table 1. Wavenumber Ranges Used for IR-Active Salts

anion	range (cm^{-1})
nitrate	1434−1267
azide	2123−1957
perchlorate	1116−1052
thiocyanide	2105−2017

All spectra were recorded *in situ* with 256 scans and 4 cm^{-1} resolution. Background spectra were recorded on the bare, dry Ge crystal in order to preserve the full water and sulfonate features in subsequent spectra. Spectra were also recorded for the multilayer buildup for both the PDADMA/PSS and for P4VMP/PSS PEMUs. The mole ratio of water to sulfonate was determined from the area under the respective peaks (range from 3706 to 2979 cm^{-1} for water and from 1052 to 989 cm^{-1} for sulfonate; for IR-active salts, see Table 1). To calibrate instrument response to H_2O and salts, a 1.00 M solution of PSS (mole ratio of water to sulfonate of 55.6) plus 0.50 M salt was passed over the uncoated crystal. Using the sulfonate signal as a convenient internal standard normalizes out differences in absolute absorbance intensities of water that result from changes in refractive indices of the multilayer. The temperature for all experiments was 23 ± 1 °C.

Results and Discussion

***In Situ* Buildup.** In the multilayering method of preparing PEC films it is known that, for a given pair of polyelectrolytes, the use of higher salt concentrations,[12] or more hydrophobic salts at the same concentration,[14] yields thicker films. A strong dependence of polyelectrolyte hydrophobicity on thickness is also observed. The mechanism of buildup is a combination of thermodynamic and kinetic factors.[23] Charge overcompensation of the "top layer" of polyelectrolyte by the adsorbing polymer is driven by thermodynamics, but the range, l_{cp}, that this overcompensation penetrates into the multilayer, which determines the amount absorbed on each cycle, is controlled by the rate of diffusion of the polymer into the film.[29] Doping (eq 1), a thermodynamic parameter, provides sites (defects) that accelerate the diffusion in a strongly nonlinear fashion,[28,31,32] which increases l_{cp}. Some polyelectrolyte combinations are so hydrophilic that they are easily doped and l_{cp} is always greater than the film thickness. Such multilayers grow exponentially.[33]

The dependence of film buildup rate on salt and polyelectrolyte type, monitored by FTIR-ATR, is illustrated in Figure 2. In the upper panel of Figure 2, the buildup of a PDADMA/PSS multilayer is depicted. The polyelectrolytes were assembled in 1.0 M solutions of NaCl, LiCl, or KCl. An oscillating pattern in the (strong) sulfonate signal is observed, similar to previously reported ATR-FTIR work.[34] Whenever an odd (PDADMA) layer is added, the sulfonate band intensity decreases, whereas

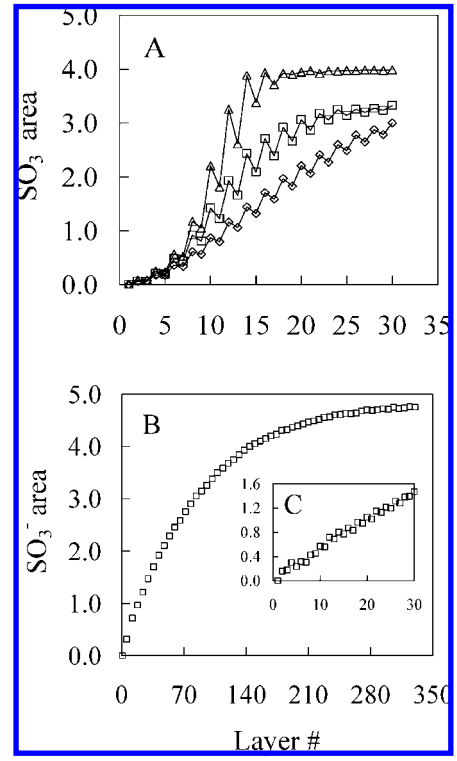

Figure 2. Sulfonate peak area vs number of layers during multilayer buildup. Panel A shows PDADMA/PSS assembled from solution containing 10 mM polymer and 1.0 M salt: △, KCl; □, NaCl; ◇, LiCl. Panel B shows the buildup of P4VMP/PSS from 1.0 M NaCl. Inset C shows the first 30 layers of P4VMP/PSS. Odd layers correspond to additions of PDADMA or P4VMP, while the even ones correspond to PSS layers.

one would expect the sulfonate absorption band to remain unchanged, since PDADMA contains no SO_3^-. In fact, when a PDADMA layer is added, the PEMU swells, taking more SO_3^- groups farther from the ATR crystal, where they are sampled more weakly by the evanescent IR wave. Oscillations in water content in PEMUs during buildup[35] have been attributed to a surface charge effect.[36] It is more accurately described as an oscillation in hydration of the outer layer: when the outer layer (of thickness l_{cp}) comprises excess PDADMA compensated by chloride ions, it is more hydrated than PSS balanced with Na^+ ions.

With a sufficient number of layers, the PEMU is thick enough to entirely contain the evanescent wave, hence no additional signal is observed, though the multilayer is still growing linearly. The fact that the oscillations also cease is consistent with the claim that they are from PEMU surface effects. For PDADMA/PSS grown in 1.0 M NaCl, we calculate an evanescent wave penetration depth of about 600 nm at the SO_3^- wavelength.[16] The dry thickness of the $(PDADMA/PSS)_{15}$ in 1 M NaCl (i.e., "30 layers") was 980 nm, which would yield a wet thickness of about 2 μm.[26,37]

In the alkali metal series Li^+, Na^+, K^+, lithium ion is the most hydrated while potassium is the least. K^+ is therefore the

(31) Ibarz, G.; Daehne, L.; Donath, E.; Möhwald, H. *Chem. Mater.* **2002**, *14*, 4059–4062.
(32) McAloney, R. A.; Dudnik, V.; Goh, M. C. *Langmuir* **2003**, *19*, 3947–3952.
(33) (a) Elbert, D. L.; Herbert, C. B.; Hubbell, J. A. *Langmuir* **1999**, *15*, 5355–5362. (b) Lavalle, P.; Gergely, C.; Cuisinier, F. J. G.; Decher, G.; Schaaf, P.; Voegel, J. C.; Picart, C. *Macromolecules* **2002**, *35*, 4458–4465. (c) Schoeler, B.; Poptoshev, E.; Caruso, F. *Macromolecules* **2003**, *36*, 5258–5264. (d) Hubsch, E.; Ball, V.; Senger, B.; Decher, G.; Voegel, J. C.; Schaaf, P. *Langmuir* **2004**, *20*, 1980–1985. (e) Lavalle, P.; Picart, C.; Mutterer, J.; Gergely, C.; Reiss, H.; Voegel, J. C.; Senger, B.; Schaaf, P. *J. Phys. Chem. B* **2004**, *108*, 635–648. (f) Laugel, N.; Betscha, C.; Winterhalter, M.; Voegel, J. C.; Schaaf, P.; Ball, V. *J. Phys. Chem. B* **2006**, *110*, 19443–19449. (g) Porcel, C.; Lavalle, P.; Ball, V.; Decher, G.; Senger, B.; Voegel, J. C.; Schaaf, P. *Langmuir* **2006**, *22*, 4376–4383.
(34) Müller, M.; Brissova, M.; Rieser, T.; Powers, A. C.; Lunkwitz, K. *Mater. Sci. Eng. C* **1999**, *8*−*9*, 163–169.
(35) McCormick, M.; Smith, R. N.; Graf, R.; Barrett, C. J.; Reven, L.; Spiess, H. W. *Macromolecules* **2003**, *36*, 3616–3625.
(36) (a) Schwarz, B.; Schönhoff, M. *Langmuir* **2002**, *18*, 2964–2966. (b) Schönhoff, M.; Ball, V.; Bausch, A. R.; Dejugnat, C.; Delorme, N.; Glinel, K.; von Klitzing, R.; Steitz, R. *Colloids Surf., A* **2007**, *303*, 14–29.
(37) (a) Jaber, J. A.; Schlenoff, J. B. *Curr. Opin. Colloid Interface Sci.* **2006**, *11*, 324–329. (b) Jaber, J. A.; Schlenoff, J. B. *Langmuir* **2007**, *23*, 896–901.

most effective at swelling the PEMU (see below), providing thicker films. The amount of oscillation seen in Figure 2A depends on the thickness of each "layer": since KCl gives thicker layers, there is a greater change when PDADMA is adsorbed. PDADMA is compensated by Cl^- in all cases. It may be possible to use "hydration matched" salts where Pol^+A^- and Pol^-M^+ are equally hydrated, which should reduce or eliminate the oscillations.

Figure 2B shows that a more hydrophobic polyelectrolyte couple, P4VMP/PSS, grows much more slowly than PDADMA/PSS in 1.0 M NaCl, which dopes the former PEMU to a much lesser degree. Each "layer" is much thinner, as polyelectrolyte cannot diffuse as far into the multilayer. Since the layers are thinner, the oscillations are also less prominent, as shown in the inset (panel C).

Doping Equilibrium. The term "doping" is used to describe the thermodynamically reversible addition of extrinsic charge (counterions) to the PEC by adding salt to the solution,[15] which is the reverse of eq 1. The most striking effect of doping is on the transport of ionic charge through the PEC.[16] For the ultrathin PEMU morphology, doping is rapid and reversible, suggesting devices can be constructed from them.[38] Doping also impacts properties such as bulk modulus, volume, adhesion (e.g., cellular adhesion), and stability of PEMUs. If one of the polyelectrolytes is a weak acid/base, solution pH also controls doping.

For a uniunivalent salt, such as NaCl, doping is described by the following equilibrium:[15,16]

$$K_{dop} = \frac{y^2}{(1-y)a_{MA}^2} \Rightarrow \frac{y^2}{a_{MA}^2} \quad \text{as } y \to 0, \quad \text{i.e., } y \sim a_{MA} \qquad (2)$$

where y is the doping level or the fraction of Pol^+Pol^- converted to Pol^+A^- and Pol^-M^+ at a particular salt, MA, concentration. y and $1 - y$ are the respective fractions of extrinsic and intrinsic charge compensation. K_{dop}^{-1} is the association constant, K_{assoc} (i.e., PEMU/salt combinations with low K_{dop} are strongly associated).

According to eq 2, an as-made PEMU, which commonly experiences a thorough rinse in distilled water at the end of an assembly, should contain no extrinsic charge (i.e., no counterions). Because of the kinetic contributions to the layering process, residual counterions are, in fact, found in PEMUs. Annealing[28,32] PEMUs in salt solutions allows most of the trapped extrinsic sites to diffuse out of the film as the polyelectrolytes slowly intermingle. Thus, we routinely annealed our multilayers in 1.0 M NaCl for at least 24 h to induce the lowest energy configuration. Annealing also reduces the surface energy of a PEMU by smoothing out the interface between the PEMU and the aqueous solution.[28,32,39]

In prior work, doping of various PEMUs was indirectly assessed by following dimensional changes using atomic force microscopy, since doping also induces swelling in the multilayer.[28] In order to directly visualize doping using ATR-FTIR, IR-active counterions must be employed. In the present case, we selected the sodium salts of azide (N_3^-), perchlorate (ClO_4^-), nitrate (NO_3^-), and thiocyanide (SCN^-). Concentrations of stock solutions were determined precisely from conductivity measurements. Mean ion activity coefficients for perchlorate, nitrate, and thiocyanide are widely accessible, while those for azide

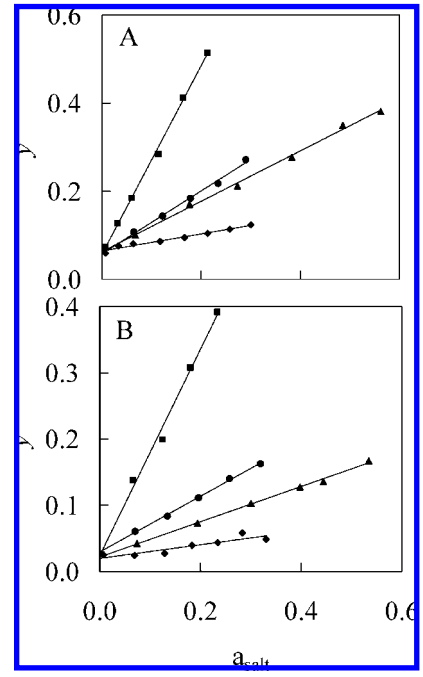

Figure 3. Mole ratio of salt/sulfonate, representing the fraction of extrinsic sites or doping level, y, for each of the IR-active ions versus solution activity of the salts: ■, perchlorate; ●, thiocyanide;▲, nitrate; ◆, azide. Panel A, $(PDADMA/PSS)_{12.5}$; panel B, $(P4VMP/PSS)_{167.5}$.

Table 2. K_{dop} and $y_{residual}$ Determined from Figure 3, and ΔG_{assoc}, Calculated from $\Delta G_{assoc} = RT \ln K_{dop}$

salt	K_{dop}	$y_{residual}$	ΔG_{assoc} (kJ mol^{-1})
	PDADMA/PSS		
$NaClO_4$	3.8	0.06	3.3
NaSCN	0.42	0.05	−2.1
$NaNO_3$	0.27	0.06	−3.2
NaN_3	0.031	0.06	−8.6
	P4VMP/PSS		
$NaClO_4$	2.9	0.02	2.6
NaSCN	0.18	0.03	−4.2
$NaNO_3$	0.071	0.02	−6.6
NaN_3	0.011	0.02	−11

are more elusive and were approximated using nitrate coefficients. In the doping process, cations and anions enter the PEMU in equal numbers, and therefore the multilayer concentration of Na^+ may be inferred. The thickness of the multilayer was sufficient to entirely contain the evanescent IR wave (the choice of a high refractive index ATR crystal helps in this respect). No solution species are "observed".

The exercise of "counting" species in multilayers containing PSS is straightforward and employs the strong SO_3^- signal as a convenient internal standard. A concentrated solution of salt and PSS served to calibrate the instrument. The value of y is simply the relative PEMU concentrations of salt and SO_3^-, $[salt]_m/[SO_3^-]_m$.

Figure 3 compares the room-temperature doping of PDADMA/PSS and P4VMP/PSS by the four salts. For small values of y (<0.4), the doping is reasonably linear with salt activity (concentration), and the slopes at low y may be used to determine K_{dop} (summarized in Table 2). The trend ClO_4^-, NO_3^-, and SCN^- follows their order in the Hofmeister series.[19,20] In order to compare relative "hydrophobicities" of ions, some literature values for hydration numbers are presented in Table 3. The ions ClO_4^-, NO_3^-, and SCN^- also follow the

(38) Salloum, D. S.; Schlenoff, J. B. *Electrochem. Solid-State Lett.* **2004**, *7*, E45–E47.
(39) Leporatti, S.; Gao, C.; Voigt, A.; Donath, E.; Möhwald, H. *Eur. Phys. J. E* **2001**, *5*, 13–20.

Table 3. Literature Values for Hydration Numbers b_{H_2O} and c_{H_2O} for Various Ions

	hydration number (b_{H_2O} or c_{H_2O})		
ion	ref 40	ref 41	ref 42
Na^+	3.5	4.5	2.1
Li^+	5.2	4.0	3.2
Mg^{2+}	10.0	10.0	9.0
Ca^{2+}	7.2	9.0	
K^+	2.6	3.5	1.1
Cs^+	2.1	2.5	1.1
Y^{3+}	14.4		
Cl^-	2.0	2.0	1.4
F^-	2.7	4.0	2.2
I^-	1.6	1.5	1.1
Br^-	1.9	1.8	
N_3^-	1.9		
SCN^-	1.7		
ClO_4^-	1.4		
NO_3^-	2.0		

hydration number trends. Azide does not follow the trend, as, according to Table 3, it should fall between nitrate and thiocyanide. However, the subjective nature of solution hydration numbers should be emphasized: classically, this number depends on the method used to determine it. For example, there is agreement between refs 40 and 41 on the hydration numbers for Mg^{2+}, Cl^-, I^-, and Br^-, but there is substantial disagreement on Na^+, Li^+, Ca^{2+}, and F^- and even more divergence with the numbers from ref 42.

Contrary to the implication of eq 2, the intercept of the doping plots is not $y = 0$. On average, PDADMA/PSS and P4VMP/PSS PEMUs show respective y intercepts of 6% and 2%, in spite of extensive annealing. At present, we are unsure whether the explanation is kinetic or thermodynamic. The former mechanism would posit that extrinsic sites are trapped kinetically as the salt concentration is lowered; that is, the interdiffusion of polyelectrolytes is so low that they cannot adopt fully intrinsic compensation. On the other hand, the plots are not curved, and even at higher salt concentrations they extrapolate to nonzero y values, $y_{residual}$. The fact that ΔH is close, but not equal, to zero may suggest that interactions between PDADMA and anions are greater than those between PSS and cations and the multilayer therefore does not contain exactly equal molar ratios of PDADMA and PSS (i.e., the bulk ratio is 1.06 for PDADMA/PSS). We are currently trying to establish whether there is an imbalance of polyelectrolytes. Nevertheless, this imbalance should not affect the doping equilibria as long as the residual is subtracted.

PEMU Hydration Equilibrium. The ATR-FTIR method provides very strong signals for water within PEMUs. We now explicitly consider PEMU water uptake in doping and compare the behavior to the level of solution hydration. Hydration of each component in the PEMU/salt system may be represented as follows:

$$n\mathrm{Pol}^+\mathrm{Pol}^-\cdot i\mathrm{H_2O_m} + \mathrm{M}^{n+}\cdot b\mathrm{H_2O_{aq}} + n\mathrm{A}^-\cdot c\mathrm{H_2O_{aq}} \rightarrow n\mathrm{Pol}^+\mathrm{A}^-\cdot d\mathrm{H_2O_m} + \mathrm{Pol}_n^-\mathrm{M}^{n+}\cdot e\mathrm{H_2O_m} + f\mathrm{H_2O_{aq}} \quad (3)$$

where M^{n+} and A^- are salt cation and anion, respectively; i, b, and c are the numbers of water molecules hydrating the intrinsic ion pair, the cation in solution, and the anion in solution, respectively; d and e are the waters hydrating the respective extrinsic ion pairs; and f represents the balance of water molecules (and can be negative or positive).

The number of water molecules associated with an ion in solution (b and c in eq 3) depends on the method of measurement and whether one differentiates between "strongly" or "weakly" bound water[42] (i.e., inner and outer coordination sphere). Since the method used here leaves no ambiguity in the number of water molecules in the condensed PEC phase, we are able to present a quantitative and general measure of PEMU hydration by different salt ions. To do so, we define a hydration coefficient, $\Pi_{salt}^{H_2O}$, for each multilayer/salt combination,

$$\Pi_{salt}^{H_2O} = \frac{r_{H_2O} - i}{[MA_n]} \quad (4)$$

Since PSS is common to both our PEMUs, r is the molar ratio of total water in the multilayer to SO_3^-, $[H_2O]/[SO_3^-]$ (standardization is performed with an aqueous solution of PSS). $\Pi_{salt}^{H_2O}$ is the slope of r vs $[MA_n]$ and is thus a simple way of expressing the effectiveness of a particular salt in hydrating a particular multilayer. The intrinsic water content of the multilayer is obtained by extrapolating back to $[MA_n] = 0$.

A complication exists from the residual extrinsic charge y_{rec} remaining in PEMUs as $[MA_n] \rightarrow 0$ (shown in Figure 3). y_{rec} induces a high osmotic pressure and brings additional water into the multilayer, yielding an upturn in the water content at low $[MA_n]$. The phenomenon is addressed in more detail later, but for the present purposes the data in Figure 4 depicts representative hydration behavior for almost all of the multilayer/salt systems we have explored. At low salt concentration, water is withdrawn from the PEMU as $[MA_n]$ increases. The film shrinks (the "polyelectrolyte effect"). As $[MA_n]$ increases further, the film is doped, the ions bring in more water, and the PEMU hydrates and expands (the "antipolyelectrolyte effect"). The solid line is the sum of the two effects. Since the polyelectrolyte effect is minimized at higher salt concentrations, extrapolation from these concentrations yields reliable values of i. Figure 4 is also useful for breaking down the contributions of intrinsic (i_{H_2O}) and extrinsic ($d_{H_2O} + e_{H_2O}$) water to the total water content (r) as a function of doping level. At doping level y, the former is $(1 - y)i$ and the latter is $(d + e)y$.

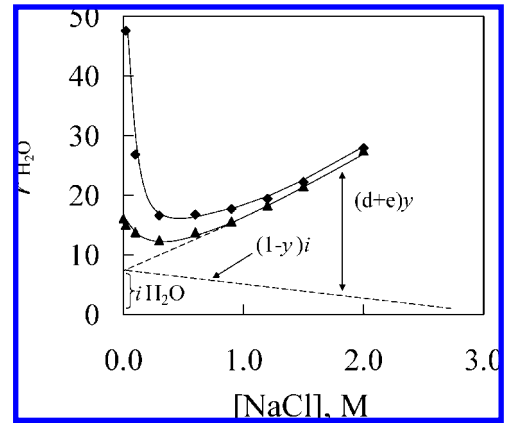

Figure 4. Number of water molecules per ion pair (r) versus NaCl concentration for a PDADMA/PSS multilayer. The upper curve represents the first run of a freshly prepared multilayer, and the lower curve represents the second and subsequent runs. The dashed lines show how the total multilayer water is broken down into intrinsic and extrinsic contributions.

(40) Marcus, Y. In *Liquid liquid interfaces: theory and methods*; Volkov, A. G., Deamer, D. W., Eds.; CRC Press: Boca Raton, FL, 1996.
(41) Bockris, J. O. M.; Saluja, P. P. S. *J. Phys. Chem.* **1972**, *76*, 2140–2151.
(42) Hasted, J. B. *Studies in Chemical Physics: Aqueous Dielectrics*; Chapman and Hall: London, 1973.

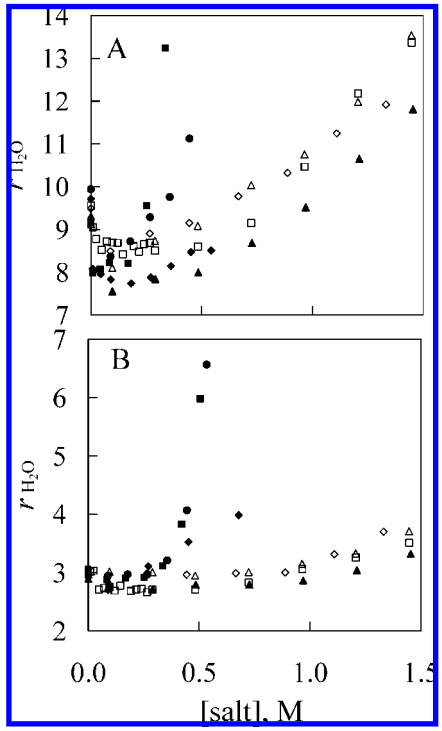

Figure 5. Number of water molecules per ion pair in PDADMA/PSS (panel A) and P4VMP/PSS (panel B) multilayers vs salt concentration for ■, $NaClO_4$; ●, NaSCN; ◇, LiCl; △, KCl; □, NaCl; ◆, NaN_3; and ▲, $NaNO_3$.

Table 4. Hydration Coefficient, $\Pi_{salt}^{H_2O}$, for Various Salts for PEMUs Built from PSS and Either PDADMA or P4VMP[a]

	$\Pi_{salt}^{H_2O}$	
salt	PDADMA	P4VMP
NaF	−5.2	−0.05
NaCl	3.8	0.63
NaBr	5.1	1.9
NaI	19.8	4.6
$NaNO_3$	3.5	0.65
$NaClO_4$	17.9	6.1
NaSCN	8.2	5.2
NaN_3	4.5	0.72
KCl	4.3	0.77
CsCl	5.8	1.5
LiCl	2.4	0.79
YCl_3	9.3	5.2
$CaCl_2$	22.3	9.4
$MgCl_2$	11.1	6.8

[a] The number of water molecules per undoped polymer ion pair, i_{H_2O}, for all salts used except NaF was 6.9 ± 1.7 for PDADMA/PSS and 2.5 ± 0.6 for P4VMP/PSS multilayers.

Figure 5 shows r as a function of $[MA_n]$ for a variety of salts. While the plots are somewhat crowded (additional data are provided in Supporting Information), the trend sketched in Figure 4 is clear. Values of $\Pi_{salt}^{H_2O}$ for the two multilayers are summarized in Table 4. Data from fluoride salts were aberrant and therefore not included in further treatments. The average values of i for PDADMA/PSS and P4VMP/PSS are 6.9 ± 1.7 and 2.5 ± 0.6, respectively, showing that P4VMP is a more "hydrophobic" PEMU. We recommend that the value of i be used as a "hydrophobicity index" for multilayers (lower i means more hydrophobic).

We investigated whether there was any evidence for a dependence of water content on PEMU thickness by comparing

Table 5. $\Pi_{salt}^{H_2O}$ Ranked for Anions and Cations and Compared with the Hofmeister Series and the Hydration Number Series (from Table 3)

$\Pi_{salt}^{H_2O}$	$ClO_4^- > I^- > SCN^- > Cl^- \approx Br^- \approx NO_3^- > N_3^-$ $Y^{3+} > Ca^{2+} > Mg^{2+} > Na^+ > K^+ > Cs^+ > Li^+$
Hofmeister	$ClO_4^- > SCN^- > I^- > NO_3^- > Br^- > Cl^-$ $Mg^{2+} > Ca^{2+} > Na^+ > K^+ > Rb^+ > Cs^+$
c_{H_2O} b_{H_2O}	$ClO_4^- < SCN^- < I^- < Br^- \sim N_3^- < NO_3^- \approx Cl^-$ $Y^{3+} > Mg^{2+} > Ca^{2+} > Li^+ > Na^+ > K^+ > Cs^+$

Table 6. Values for $d_{H2O} + e_{H2O}$ of IR-Active Ions Doping PDADMA/PSS and P4VMP/PSS Multilayers

	$(d+e)_{H_2O}$	
ion−polymer pair	PDADMA/PSS	P4VMP/PSS
$Pol^- Na^+$, $Pol^+ ClO_4^-$	9.3	6.7
$Pol^- Na^+$, $Pol^+ SCN^-$	9.5	8.3
$Pol^- Na^+$, $Pol^+ NO_3^-$	10.6	8.5
$Pol^- Na^+$, $Pol^+ N_3^-$	11.6	8.8

i for PDADMA/PSS films of thickness 20, 26, 32, and 40 layers. The value of i was the same within experimental error (6.4 ± 0.5).

The order of $\Pi_{salt}^{H_2O}$ values (Table 4) follows the solution hydration trend in reverse. In other words, the less hydrated in solution, the more effective an ion is at hydrating the PEMU for a given concentration. Such a trend is a consequence of significantly better doping by less hydrated ions. The comparison is best made, of course, between ions of the same charge. The "salting out" trend for biopolymers, noted by Hofmeister,[19,43] is compared to the PEMU hydration coefficients for some of the ions in Table 5. A couple of ions are slightly out of order. Also included in Table 5 is the hydration trend from Table 3. The "hydration series" (i.e., b_{H_2O} and c_{H_2O}) describes the trend as well as the Hofmeister series. The hydration numbers show very small differences between those ions that are out of order, except Ca^{2+} and Mg^{2+}.

The influence of different salts on the aqueous solution properties of small and large molecules is often rationalized in terms of effects on water structure. The concepts of "structure making" (kosmotropic) and "structure breaking" (chaotropic)[20,44] of water by various ions were not part of the original work by Hofmeister (he was more concerned with disruption of the digestive system than of water structure!). Such terminology evolved later as researchers began to ponder the special hydrogen-bonding interactions of water. It is now standard practice to use these concepts in rationalizing hydrophobic interactions.

Indications of changes in the structure of water, particularly those changes that impact the degree of hydrogen bonding, are traditionally observed from vibrational spectroscopy.[6,45] We compared the IR spectra of the water O−H stretching region in bulk water, a multilayer with intrinsic water, and a multilayer

(43) Salomäki, M.; Tervasmäki, P.; Areva, S.; Kankare, J. *Langmuir* **2004**, *20*, 3679–3683.
(44) (a) Leberman, R. *FEBS Lett.* **1991**, *284*, 293–294. (b) Leontidis, E. *Curr. Opin. Colloid Interface Sci.* **2002**, *7*, 81–91.
(45) (a) Terada, T.; Maeda, Y.; Kitano, H. *J. Phys. Chem.* **1993**, *97*, 3619–3622. (b) Kitano, H.; Imai, M.; Sudo, K.; Ide, M. *J. Phys. Chem. B* **2002**, *106*, 11391–11396. (c) Kitano, H.; Imai, M.; Mori, T.; Gemmei-Ide, M.; Yokoyama, Y.; Ishihara, K. *Langmuir* **2003**, *19*, 10260–10266. (d) Thouvenin, M.; Linossier, I.; Sire, O.; Peron, J.-J.; Vallee-Rehel, K. *Macromolecules* **2002**, *35*, 489–498.

doped at $y \approx 0.5$ with a hydrophobic ion (perchlorate) and a more hydrophilic ion (nitrate). No significant differences could be discerned in the shape of the water spectrum (see Supporting Information). For comparison, in Figure 6 we follow the "brute force" removal of water from a multilayer by drying it. Because the signal from liquid water bands is distorted by the omnipresent water vapor absorption in the optical path, D_2O was employed for this experiment. As expected, when hydrogen (deuterium) bonds are removed, the absorption shifts to higher energy, but only when the water becomes quite diluted, suggesting a robust ability of water to maintain a H-bonding network within the PEMU matrix. Finney, using neutron scattering, finds no evidence for greater ordering of hydration water around a solute than bulk water.[1]

Toward a Universal Doping Parameter. Using the breakdown of r_{H_2O} shown in Figure 4, we are able to determine the hydration of extrinsic sites ($d + e$ water in eq 3). Table 6 summarizes our findings for ($d + e$) in the two multilayers studied here. While the sum $d + e$ is accurately known, the individual hydration levels of Pol^+A^- and Pol^-M^+ are not, although it is clear from Figure 2 that $d > e$.

If φ is the equilibrium constant that explicitly recognizes water of hydration, as in eq 3, then

$$\varphi = \frac{y^2}{(1-y)a_{MA}^2} \frac{a_{H_2O,m}^d a_{H_2O,m}^e}{a_{H_2O,m}^i} \tag{5}$$

Water in the dilute aqueous phase approximates pure water and is, as routine practice, assigned an activity = 1.

$$\text{Let} \qquad z = (d+e) - i \tag{6}$$

i.e., z is the number of water molecules released from the polymer repeat units when an ion pair is formed. Then

$$\varphi = K_{dop} a_{H_2O,m}^z \tag{7}$$

Total water in the multilayer is the sum of the intrinsic water and the extrinsic water, which depends on the doping level (as illustrated in Figure 4):

$$a_{H_2O,m} = \left(\frac{d+e}{V_m}\right) y + \frac{i}{V_m}(1-y) = \frac{zy+i}{V_m} \tag{8}$$

where V_m is the molar volume of the multilayer. Thus,

$$\varphi = K_{dop}\left(\frac{zy+i}{V_m}\right)^z \qquad \text{or} \qquad \varphi = K_{dop}\left(\frac{i}{V_m}\right)_{y\to 0}^z \tag{9}$$

We now present the following thesis: given that the association between polyelectrolytes is "ideal" (net entropy driven), proper counting of all species transferring between the multilayer and aqueous phase should account completely for energy changes. When polyelectrolytes associate in the presence of uni-univalent salt (e.g., NaCl) they all undergo similar ion-exchange-type reactions such as that shown in eq 3. For $\Delta H = 0$, the difference is only in the redistribution of water that accompanies the exchange. In our experiments, water molecules are counted directly. Thus, for *any* combination of M^+ and A^-,

$$\varphi_{y\to 0, \Delta H \to 0} = \text{constant} \tag{10}$$

We emphasize that our approach is not based on a fundamental evaluation of specific inter- and intramolecular interactions, such as dipolar forces, hydrogen bonding, induced dipoles, dielectric constant fluctuations, or any such interactions that are the subject of numerous elegant theoretical studies. We are merely observing water molecules that function as "reporters" of the net results of these interactions. Our definition of hydrophobicity is "visualized" in that a more hydrophobic system will simply be less hydrated. Unambiguous counting and tracking of water molecules is possible in the experimental system described here.

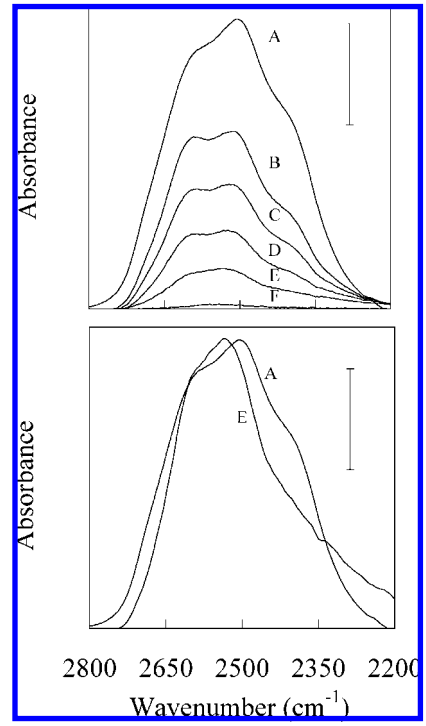

Figure 6. O−D stretching region from ATR-FTIR of a $(PDADMA/PSS)_{12.5}$ PEMU as it is dried under a stream of N_2. Upper panel: multilayer is converted from fully hydrated (A, $r = 11$; B, $r = 7$; C, $r = 4$; D, $r = 2$; E, $r = 0.7$; F, $r = 0.1$); scale bar is 0.07 AU. Lower panel: curve E has been normalized to curve A to illustrate the difference in shape; scale bar is 0.07 AU for curve A and 0.014 for curve E ($r = 0.7$).

The utility of our thesis is that the hydrophobicity of the two counterion-compensated polyelectrolyte repeat units *and* that of the polyelectrolyte/polyelectrolyte ion pair are represented by respective values for $d + e$ and i. To compare different multilayers, it is useful to employ a reference PEMU such that

$$K_{dop}\left(\frac{i}{V_m}\right)_{y\to 0}^z = K_{dop,ref}\left(\frac{i_{ref}}{V_{ref}}\right)_{y\to 0}^{z_{ref}} \tag{11}$$

where $K_{dop,ref}$, V_{ref}, and z_{ref} are quantities for the reference multilayer. We have shown that $NaNO_3$-doped PDADMA/PSS approaches $\Delta H = 0$.[10] Using a V_{ref} for this PEMU of 0.405 L, $d + e = 10.6$ (Table 6), $i = 6.9$, $z_{ref} = 3.7$, and $K_{dop,ref} = 0.27$ (Table 2), we may write

$$K_{dop} = \Psi\left(\frac{V_m}{i}\right)^z \qquad \text{as } y \to 0 \tag{12}$$

Ψ, which can be considered a universal parameter for all polyelectrolyte complexes that associate in any uni-univalent salt MA with $\Delta H = 0$, has a value of about 9700. The formation energy per ion pair, Δg, is not high. For example, $\Delta g = (9.13 - 2.8z)kT$ and $(9.13 - 2.1z)kT$ for PDADMA/PSS and P4VMP/PSS ion pairing, respectively.

Equation 12 captures the experimental findings that more hydrophobic polyelectrolyte pairs are harder to dope, or swell (since i is smaller, z is larger), while more hydrophobic

Table 7. Values of i, $d + e$, z, V_m, and Corresponding Calculated $K_{dop,calc}$ (from Eq 12) and ΔH_{dop} (from Eq 13)[a]

salt	i	$(d + e)$	z	V_m	$K_{dop,\ calc}$	ΔH_{dop} (kJ/mol)	ΔG_{dop}[c] (kJ/mol)
				PDADMA/PSS			
$NaClO_4$	6.9	9.3	2.4	0.405	11	2	−5.9
NaSCN	6.9	9.5	2.6	0.405	6	7	−4.4
$NaNO_3$	6.9	10.6	3.7	0.405	-	0	-
NaN_3	6.9	11.6	4.7	0.405	0.02	−1	+9.6
NaCl	6.9	11.6[b]	3.7[b]	0.405	0.27	-	+3.2
NaBr	6.9	10.5[b]	3.6[b]	0.405	0.4	-	+2.3
NaI	6.9	10.2[b]	3.3[b]	0.405	0.8	-	+0.6
LiCl	6.9	12.3[b]	5.4[b]	0.405	0.002	-	+15.3
KCl	6.9	9.7[b]	2.8[b]	0.405	4	-	−3.4
CsCl	6.9	9.2[b]	2.3[b]	0.405	14	-	−6.5
				P4VMP/PSS			
$NaClO_4$	2.5	6.7	4.2	0.313	2	−1	−1.7
NaSCN	2.5	8.3	5.8	0.313	0.06	−3	+6.8
$NaNO_3$	2.5	8.5	6	0.313	0.04	−1	+7.9
NaN_3	2.5	8.8	6.3	0.313	0.02	1	+9.6
NaCl	2.5	8.5[b]	6[b]	0.313	0.04	-	+7.9
NaBr	2.5	8.4[b]	5.9[b]	0.313	0.05	-	+7.3
NaI	2.5	8.1[b]	5.6[b]	0.313	0.09	-	+5.9
LiCl	2.5	10.2[b]	7.7[b]	0.313	0.001	-	+17
KCl	2.5	7.6[b]	5.1[b]	0.313	0.2	-	+3.4
CsCl	2.5	7.1[b]	4.6[b]	0.313	0.7	-	+0.9

[a] Estimated values based on eq 14. [b] +3.2 kJ experimental. [c] High positive ΔG means it requires a high salt concentration to dope.

counterions are more effective dopants ($d + e$ is smaller, which makes z smaller for constant i). It also shows that polyelectrolyte complexes of low V_m, such as poly(allylamine)/PSS (high "charge density", although electrostatics does not come into our treatment), are more difficult to dope. Values for K_{dop} are given in Table 7, calculated using a V_m for P4MVP/PSS of 0.313 L. The rough agreement with measured values in Table 2 is reasonable, considering the large influence of a small error in z (eq 12).

A slight difference in hydration has a significant impact on ΔG. If ΔH is minimal, then clearly hydration number is the dominant driving force. The contribution of ΔH, which must be measured by sensitive calorimetric methods (such as isothermal calorimetry[10,46]), can be estimated as follows:

$$\Delta H_{dop} = RT \ln K_{dop,calc} - RT \ln K_{dop} \qquad (13)$$

We include a rough estimate of ΔH_{dop} in Table 7. Small endothermic or exothermic enthalpies of doping are indicated. Of course, our perspective is on the ability of ions to dope multilayers. The corresponding enthalpy of association, ΔH_{assoc}, would be $-\Delta H_{dop}$. Small exo- or endothermic values for ΔH_{assoc} have been measured for polyelectrolyte complexation.[10,46]

Both i and z may be determined experimentally, using ATR-FTIR, for infrared-active ions only. Unfortunately, this leaves out many common salts, including NaCl, which is almost universally employed for multilayers. However, we estimate K_{dop} by assuming that the additional hydration within the multilayer is the sum of the additional hydration of counterions as follows:

$$(d + e)_{MA} = (d + e)_{NaNO_3} + (b_{M^+} - b_{Na^+}) + (c_{A^-} - c_{NO_3^-}) \qquad (14)$$

Estimates of $(d + e)$ for IR-inactive salts, using sodium nitrate as the reference, and their corresponding K_{dop} are listed in Table 7. The three salts with multiply charged cations, M^{n+}, examined here (Ca^{2+}, Mg^{2+}, Y^{3+}) are highly hydrated (Table 3) and appear to contradict the arguments above: well-hydrated ions should not be able to dope or hydrate the multilayer efficiently. However, it requires fewer hydrated M^{n+} ions to produce the same doping level, leveraging the multiplicity of charge in an entropically advantageous way (cf. the "ligand effect"). In other words, yM^{n+} ions produce the same doping as nyM^+ ions. We have not measured any doping levels for these ions.

Although we have focused on polyelectrolytes complexes, recent analyses of the behavior of polyelectrolyte interactions with multivalent ions[47] have also highlighted the role of entropy as a driving force. For example, the binding of Ca^{2+} to poly(acrylic acid) was explained by release of water molecules,[47b] as was unexpectedly extensive binding of NaCl to a neutral polymer.[47c]

Swelling from Residual Extrinsic Sites: The "Polyelectrolyte Effect". Figures 4 and 5 clearly show opposing trends in water uptake at low and high salt concentration — more evident with the more hydrophilic PDADMA/PSS. The water that is extracted at low salt concentration is viewed as not being specifically associated with the polymer/polymer ion pairs (i) represented in eq 3. Additional water could be outside of the first hydration shell, or perhaps in (nano)pools or pores of water. The first salt doping curve performed on an unannealed PDADMA/PSS multilayer, shown in Figure 4, starts with exceeding high, and irreproducible, values of r. We attribute this anomalously high water content to a greater concentration of extrinsic sites, and perhaps to nanopores that are locked into the structure of the PEMU during buildup. Evidence for "pores" of about 1 nm has been observed from transport[48] and NMR[49] measurements. After one exposure of the multilayer to high salt concentration, the PEMU is annealed, the extrinsic sites are minimized, and most of the unassociated water is expelled. The second and subsequent doping curves now coincide. The high salt branch of r vs $[MA_n]$ (Figure 5 and Supporting Information) is used to determine i (and also $d + e$ for the IR-active anions).

The shapes of the curves in Figure 4 and 5 have also been observed in other polyelectrolyte systems with residual extrinsic charge. For example, polyampholytic hydrogels are made by polymerizing positive and negative monomers of precise stoichiometry.[50,51] When this stoichiometry deviates from 1.0, the residual extrinsic charge causes hydrogels to shrink upon the addition of salt at low [NaCl], followed, in some cases, by expansion at higher [NaCl]. The work of Nisato et al., in particular, shows compositions with $y_{residual}$ of ca. 5%.[51]

The standard explanation for contraction of a polyelectrolyte with increasing salt concentration invokes screening of polymer charges by salt ions.[52] In the present case, it is difficult to see how salt ions brought into the PEMU by doping can overwhelm

(46) Bharadwaj, S.; Montazeri, R.; Haynie, D. T. *Langmuir* **2006**, *22*, 6093–6101.

(47) (a) Huber, K. *J. Phys. Chem.* **1993**, *97*, 9825–9830. (b) Sinn, C. G.; Dimova, R.; Antonietti, M. *Macromolecules* **2004**, *37*, 3444–3450. (c) Sinn, C. G.; Dimova, R.; Huin, C.; Sei, O.; Antonietti, M. *Macromolecules* **2006**, *39*, 6310–6312.

(48) (a) Liu, X. Y.; Bruening, M. L. *Chem. Mater.* **2004**, *16*, 351–357. (b) Jin, W. Q.; Toutianoush, A.; Tieke, B. *Appl. Surf. Sci.* **2005**, *246*, 444–450.

(49) Vaca Chavez, F.; Schönhoff, M. *J. Chem. Phys.* **2007**, *126*, 104705.

(50) (a) Baker, J. P.; Blanch, H. W.; Prausnitz, J. M. *Polymer* **1995**, *36*, 1061–1069. (b) English, A. E.; Tanaka, T.; Edelman, E. R. *Macromolecules* **1998**, *31*, 1989–1995.

(51) Nisato, G.; Munch, J. P.; Candau, S. J. *Langmuir* **1999**, *15*, 4236–4244.

(52) Dautzenberg, H.; Jaeger, W.; Kötz, J.; Philipp, B.; Seidel, Ch.; Stscherbina, D. *Polyelectrolytes: Formation, Characterization and Application*; Hanser: Munich, 1994.

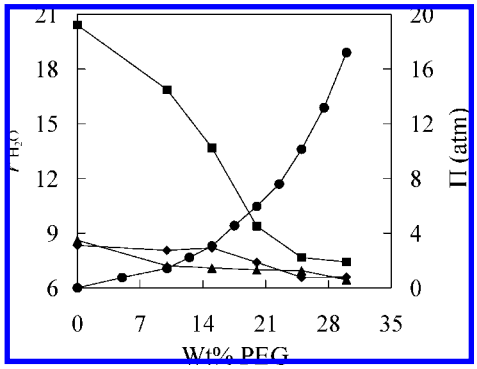

Figure 7. *r* for a PDADMA/PSS multilayer vs wt % of PEG osmotic stressing agent at room temperature: ■, multilayer in 10 mM NaCl before annealing; ◆, in 10 mM NaCl after annealing in 1.0 M NaCl for 24 h; ▲, in 0.5 M NaCl after annealing. The osmotic pressure corresponding to the PEG concentration in pure water at 20 °C is also shown (●).[54]

effects caused by a much greater population of residual intrinsic ions. Figure 3, for example, shows no significant additional counterions within the PEMU at low salt concentration. We interpret the dehydration of a multilayer at low salt concentration as a consequence of the increased osmotic pressure of the external solution.

To test the osmotic pressure hypothesis of PEMU dehydration at low salt concentration, we measured the multilayer water content with different concentrations of poly(ethylene glycol) (PEG) in the solution, maintaining a constant ionic strength. PEG is used as an osmotic stressing agent:[30,53] as a polar, hydrophilic polymer, it exerts significant osmotic pressure but does not enter the PEMU due to excluded volume restrictions. Figure 7 shows the water content of both an annealed and an unannealed PDADMA/PSS multilayer with increasing concentration of 8000 MW PEG to which 10 mM (i.e., dilute) salt is also added. The PEG solution, which generates osmotic pressures of many atmospheres, is highly effective at drawing water out of unannealed PEMU (Figure 7). When the PEMU is annealed, much less water is extractable, especially if additional salt is present in the solution (here, 0.5 M NaCl). It appears that water molecules *i*, *d*, and *e*, in eq 3 are *not* subject to osmotic pressure control, consistent with the doping relationships assumed in eqs 5−10.

(53) Leikin, S.; Parsegian, V. A.; Rau, D. C.; Rand, R. P. *Annu. Rev. Phys. Chem.* **1993**, *44*, 369–395.

Significantly, most of the water is extracted by 20 wt % PEG, at which point the osmotic pressure corresponds to that generated by 0.25 M NaCl, close to the minimum in Figure 4. We conclude that the salt-induced shrinkage in non-stoichiometric polyelectrolyte complexes is due to osmotic pressure dehydration, not to screening. Water molecules *i*, *e*, and *d* do not appear to be osmotically extractable.

Conclusions

A series of quantitative relationships have been developed for equilibria between extrinsic and intrinsic charge compensation in polyelectrolyte complexes. These are ion-pairing interactions, subject to ion-exchange-type rearrangements and driven by entropy. The participation of water molecules in these equilibria has been directly revealed by *in situ* IR spectroscopy. Proper counting of all exchanged species leads to a universal parameter for all combinations of uniunivalent salt and polyelectrolytes. No evidence of disruption of the H-bonding network during doping is indicated by vibrational spectroscopy. The fact that water retains its H-bonding network, even when it is hydrating complexes, suggests that the water is clustered around the ionic functionality. In fact, evidence for breaking H-bonds is seen only on extensive dispersion of water (by drying).

Ion-pairing ("electroneutralization") interactions are stronger when acting in cooperation rather than individually. The role of these interactions in protein folding is widely acknowledged, though usually presented in terms of electrostatics. Cursory examination of the interior of globular proteins indicates that ion-pairing interactions are distributed throughout. Ionic sites are often adjacent to more hydrophobic amino acids, which would promote association, as shown by the present work. Perhaps ion-pairing sites act as "waypoints" to guide folding over an intermediate range.

Acknowledgment. This work was supported by the National Science Foundation (grant DMR-0309441).

Supporting Information Available: IR spectra and plots of water content for various salts. This material is available free of charge via the Internet at http://pubs.acs.org.

JA802054K

(54) http://dir.nichd.nig.gov/Lpbs/docs/osmdata/osmdata.html.